

# Structural basis of drugs that increase cardiac inward rectifier Kir2.1 currents

Ricardo Gómez<sup>1†</sup>, Ricardo Caballero<sup>1,2\*†</sup>, Adriana Barana<sup>1,3</sup>, Irene Amorós<sup>1,2</sup>, Sue-Haida De Palm<sup>1</sup>, Marcos Matamoros<sup>1,2</sup>, Mercedes Núñez<sup>1,2</sup>, Marta Pérez-Hernández<sup>1,3</sup>, Isabel Iriepa<sup>4</sup>, Juan Tamargo<sup>1,3</sup>, and Eva Delpón<sup>1,2</sup>

<sup>1</sup>Department of Pharmacology, School of Medicine, Universidad Complutense, Madrid 28040, Spain; <sup>2</sup>Instituto de Investigación Sanitaria Gregorio Marañón, School of Medicine, Universidad Complutense, Madrid 28040, Spain; <sup>3</sup>Instituto de Investigación Sanitaria Hospital Clínico San Carlos, School of Medicine, Universidad Complutense, Madrid, Spain; and <sup>4</sup>Department of Organic Chemistry, School of Pharmacy, Universidad de Alcalá, Alcalá de Henares, Spain

Received 22 January 2014; revised 24 July 2014; accepted 12 August 2014

Time for primary review: 52 days

<b>Aims</b>	We hypothesize that some drugs, besides flecainide, increase the inward rectifier current ( $I_{K1}$ ) generated by Kir2.1 homotetramers ( $I_{Kir2.1}$ ) and thus, exhibit pro- and/or antiarrhythmic effects particularly at the ventricular level. To test this hypothesis, we analysed the effects of propafenone, atenolol, dronedarone, and timolol on Kir2.x channels.
<b>Methods and results</b>	Currents were recorded with the patch-clamp technique using whole-cell, inside-out, and cell-attached configurations. Propafenone (0.1 nM–1 $\mu$ M) did not modify either $I_{K1}$ recorded in human right atrial myocytes or the current generated by homo- or heterotetramers of Kir2.2 and 2.3 channels recorded in transiently transfected Chinese hamster ovary cells. On the other hand, propafenone increased $I_{Kir2.1}$ ( $EC_{50} = 12.0 \pm 3.0$ nM) as a consequence of its interaction with Cys311, an effect which decreased inward rectification of the current. Propafenone significantly increased mean open time and opening frequency at all the voltages tested, resulting in a significant increase of the mean open probability of the channel. Timolol, which interacted with Cys311, was also able to increase $I_{Kir2.1}$ . On the contrary, neither atenolol nor dronedarone modified $I_{Kir2.1}$ . Molecular modelling of the Kir2.1–drugs interaction allowed identification of the pharmacophore of drugs that increase $I_{Kir2.1}$ .
<b>Conclusions</b>	Kir2.1 channels exhibit a binding site determined by Cys311 that is responsible for drug-induced $I_{Kir2.1}$ increase. Drug binding decreases channel affinity for polyamines and current rectification, and can be a mechanism of drug-induced pro- and antiarrhythmic effects not considered until now.
<b>Keywords</b>	Propafenone • Inward rectifier channels • Dronedarone • Atenolol • $I_{K1}$

## 1. Introduction

Inward rectifier current ( $I_{K1}$ ) is the key  $K^+$  current responsible for setting the resting membrane potential, controlling excitability, and modulating late-phase repolarization and action potential duration (APD) in cardiac cells.<sup>1</sup> Human cardiac  $I_{K1}$  is generated by Kir2.x channels, which are distributed differentially between atria and ventricles. Indeed, Kir2.2 and 2.3 channel densities seem to be greater in the atria than in the ventricles, whereas the role of Kir2.1 channels seems to be greater in the ventricles.<sup>2</sup>

There are clinical and experimental data suggesting that an increase in the outward component of the  $I_{K1}$  could enhance arrhythmogenesis. It

was demonstrated that transgenic upregulation of  $I_{K1}$  in the mouse heart is proarrhythmic,<sup>3</sup> and that the greater the outward  $I_{K1}$  component, the faster and more stable the rotors that generate ventricular fibrillation in a guinea pig model.<sup>4</sup> In contrast,  $I_{K1}$  inhibition using low  $BaCl_2$  concentrations abolished the arrhythmic activity,<sup>3,5</sup> thereby illustrating that  $I_{K1}$  blockade may be a potentially useful antiarrhythmic strategy. Numerous studies have demonstrated that increased  $I_{K1}$  also enhanced fibrillatory activity in the atria both in animal models and in patients.<sup>6</sup> It has been shown that, in patients with chronic atrial fibrillation (AF), an AF-induced increase of  $I_{K1}$  is critical for the stabilization and maintenance of the arrhythmia.<sup>7</sup> Furthermore, gain-of-function mutations in the gene encoding Kir2.1 channel (KCNJ2) result in type 3 short QT syndrome

\* Corresponding author. Tel: +34 91 394 14 74; fax: +34 91 394 14 70, Email: rcaballero@med.ucm.es

† R.G. and R.C. contributed equally.

characterized by ventricular proarrhythmia frequently associated with AF.<sup>8</sup> In contrast, it has been proposed that an  $I_{K1}$  increase could stabilize the resting membrane potential inhibiting the generation of delayed afterdepolarizations (DADs).<sup>9</sup> In this setting, a drug-induced  $I_{K1}$  increase could be a useful strategy for the control of DAD-induced arrhythmias.

Recently, it has been demonstrated that flecainide, a class Ic antiarrhythmic drug widely used for the acute cardioversion of recent onset AF that exhibits ventricular proarrhythmic effects, increases the current generated by Kir2.1 homotetramers.<sup>10</sup> In contrast, flecainide neither blocks nor increases the currents generated by Kir2.2/2.3 homo and heterotetramers. Consistent with this, flecainide does not modify guinea pig and human atrial  $I_{K1}$ , while it increases guinea pig ventricular  $I_{K1}$ . This selectivity for Kir2.1 was attributed to the flecainide interaction with a cysteine residue (Cys 311), which in Kir2.2 and 2.3 channels is an Alanine (Ala).

These results led us to propose that a putative flecainide-induced increase of ventricular  $I_{K1}$  might contribute to its proarrhythmic effects. Therefore, a drug-induced  $I_{K1}$  increase could be, at least on a theoretical basis, a mechanism of drug-induced proarrhythmic effects not considered until now. The question arises now is as to whether other antiarrhythmic drugs, that also exhibit chamber-specific proarrhythmic effects, selectively increase  $I_{Kir2.1}$  by binding to Cys311. Furthermore, it would be of great interest to elucidate the chemical determinants of drug affinity to this binding site within Kir2.1 channels.

For a preliminary answer to these questions, here we analysed the effects of propafenone, another class Ic antiarrhythmic drug widely used for acute cardioversion of recent onset AF. Propafenone is chemically related with flecainide, which could contribute to the elucidation of the chemical requirements of the drug-induced Kir2.1 increasing effects. Moreover, the pharmacological profile, therapeutic indications, and ventricular proarrhythmic features of propafenone and flecainide are very similar.<sup>11</sup> We also studied the effects of atenolol and timolol, two  $\beta$ 1-adrenergic receptor antagonists which are structurally very similar to propafenone.<sup>12</sup> Finally, we tested the effects of dronedarone, a multi-channel blocker used for the prevention of recurrences of AF which neither produces ventricular proarrhythmia nor is chemically close to propafenone and flecainide.<sup>13</sup> Based on our results, we propose the pharmacophore for drugs interacting with Cys311. Overall, we demonstrate that Kir2.1 channels exhibit a binding site determined by Cys311, which is responsible for a drug-induced  $I_{Kir2.1}$  increase. Drug binding to this binding site decreases the affinity of the channel for polyamines and current rectification.

## 2. Methods

### 2.1 Human atrial and guinea pig myocyte isolation

The study in human cells was approved by the Investigation Committee of the Hospital Universitario Gregorio Marañón (CNIC-13) and conforms to the principles outlined in the Declaration of Helsinki. Each patient gave written informed consent. Human right atrial samples were obtained from patients ( $n = 4$ ) who underwent cardiac surgery (see Supplementary material online, Table S1). The animal studies were approved by the University Committee on the Use and Care of animals at the Complutense University and conform to the Guidelines from Directive 2010/63/EU of the European Parliament on the protection of animals used for scientific purposes. Human atrial and guinea pig myocytes were isolated following previously described methods.<sup>10,14</sup>

### 2.2 Kir2.x constructs and cell transfection

Chinese hamster ovary (CHO) cells were transiently transfected with the cDNA encoding wild-type (WT) or mutated Kir2.x channels together with the cDNA encoding the CD8 antigen by using FUGENE XtremeGENE (Roche Diagnostics, Switzerland) following the manufacturer's instructions. Coexpression experiments (Kir2.1/Kir2.2, Kir2.1/Kir2.3, Kir2.2/Kir2.3) were performed using an 0.5 : 0.5 ratio. Forty-eight hours after transfection, cells were incubated with polystyrene microbeads precoated with anti-CD8 antibody.<sup>10,15,16</sup>

### 2.3 Macroscopic current recordings

Macroscopic currents were recorded at room temperature (21–23°C) using the whole-cell patch-clamp technique and filtered at half the sampling frequency (micropipette resistance  $\leq 3.5$  M $\Omega$ ).<sup>10,14–16</sup> Series resistance was compensated manually and  $\geq 80\%$  compensation was achieved. Under our experimental conditions, no significant voltage errors ( $< 5$  mV) due to series resistance were expected with the micropipettes used. Current–voltage ( $I$ – $V$ ) curves were corrected according to the calculated liquid junction potential.<sup>10,15,16</sup>

### 2.4 Single-channel recordings

Single-channel currents were recorded at room temperature using the cell-attached patch-clamp configuration.<sup>10,15,16</sup> Patch pipettes (tip resistance between 5 and 10 M $\Omega$ ) were coated at the tip with Sylgard (Dow Corning, USA), and fire-polished with a microforge. Patches with more than one channel were discarded.

### 2.5 Inside-out recordings

In some experiments, currents were recorded at room temperature from excised inside-out macropatches from HEK-293 cells (micropipette resistance 1.0–1.5 M $\Omega$ ).<sup>10,16</sup> Recordings were made by using a fluoride, vanadate, and pyrophosphate-potassium solution on both sides of the patch to prevent current rundown.<sup>10,16</sup> This solution was Mg<sup>2+</sup>- and spermine-free. A solution adjusted to pH 5.0 was used to abolish any detectable currents through Kir channels. Offline subtraction of the currents recorded while perfusing with this solution was used to correct for endogenous currents.

### 2.6 Computational modelling

Molecular modelling was performed by means of Autodock Vina.<sup>17</sup> A homology model of human Kir2.1 (uniprot:p63252) was built based on the tetrameric template structure of chicken Kir2.2 (PDB ID 3SPH). CHARMM force field was applied using the receptor-ligand interactions tool in Discovery Studio, version 2.1, software package.<sup>18</sup> According to Vina best scored poses, the most stable drug-channel complex configurations were considered.

### 2.7 Drugs

Drugs were dissolved as appropriate to yield 10 mM stock solutions. Further dilutions were carried out in external solution to obtain the desired final concentration. Control solutions always contained the same solvent concentrations as the test solution.

### 2.8 Statistical methods

Results are expressed as mean  $\pm$  SEM from data obtained from 'n' experiments/cells. Paired or unpaired  $t$ -test or one-way ANOVA followed by the Newman–Keuls test were used to assess statistical significance where appropriate. To make comparisons between two different concentration–response curves, an  $F$ -test was used. A value of  $P < 0.05$  was considered significant.

A more detailed description of the experimental procedures can be found in Supplementary material.

### 3. Results

#### 3.1 Low propafenone concentrations increase Kir2.1, but not Kir2.2 and 2.3, currents

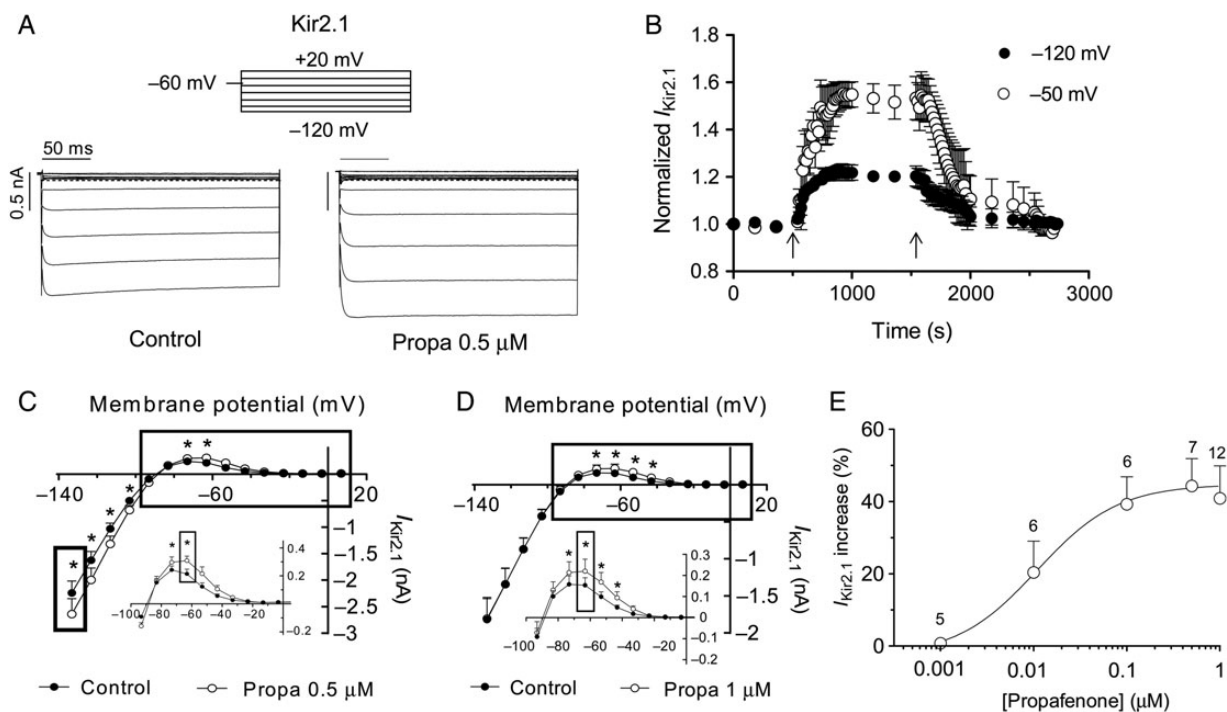
It has been recently demonstrated that propafenone inhibits the current generated by Kir2.x channels at supra-therapeutic micromolar concentrations ( $>1 \mu\text{M}$ ).<sup>16</sup> At these concentrations, the cationic form of propafenone incorporates into the cytoplasmic domain of the channel [Arginine (Arg) residues 228 and 260 in Kir2.1], thereby decreasing the net negative charge in the pore, which is sensed by  $\text{K}^+$  ions and polyamines. This effect, in turn, promotes the appearance of subconductance levels and the decrease of the channel affinity for phosphatidylinositol 4,5-bisphosphate ( $\text{PIP}_2$ ).<sup>16</sup> In contrast, the effects of low nanomolar concentrations have not been explored yet. Given the close structural similarity between propafenone and flecainide, we surmised that propafenone might also increase  $I_{Kir2.1}$  and decided to analyse the effects of low propafenone concentrations on Kir2.1 channels.

Figure 1A shows  $I_{Kir2.1}$  traces recorded in a CHO cell transiently transfected with Kir2.1 channels by applying 250 ms pulses from a holding potential of  $-60 \text{ mV}$  to potentials ranging from  $-120$  to  $+20 \text{ mV}$  under control conditions and in the presence of  $0.5 \mu\text{M}$  propafenone. Although propafenone significantly increased both inward ( $19.0 \pm 1.9\%$  at  $-120 \text{ mV}$ ) and outward  $I_{Kir2.1}$  ( $44.3 \pm 7.6\%$  at  $-50 \text{ mV}$ ,  $n = 7$ ; Figure 1A and C), the effects on outward  $I_{Kir2.1}$  were greater than those

on inward current. In any case, increasing effects were completely reversible upon washout (Figure 1B). Supplementary material online, Figure S1 shows the increasing and inhibiting effects produced by propafenone in a wide range of concentrations ( $0.001$ – $100 \mu\text{M}$ ) at  $-120$  and  $-50 \text{ mV}$ . The results demonstrated that, for a given concentration, propafenone-induced increase was always more marked at potentials positive to the  $E_K$ , which are the physiologically relevant, than at potentials negative to the  $E_K$ . In fact, only two propafenone concentrations actually increased the current at negative potentials. Moreover, at some concentrations such as  $1$ ,  $5$ , and  $10 \mu\text{M}$ , propafenone increased the current at  $-50 \text{ mV}$  while it either did not modify (Figure 1D and see Supplementary material online, Figure S1) or even decreased the current at  $-120 \text{ mV}$ . Figure 1E shows the concentration-dependence of the propafenone  $I_{Kir2.1}$  increasing effects at  $-50 \text{ mV}$ . The  $\text{EC}_{50}$  and the maximum effect ( $E_{\text{max}}$ ) were calculated by fitting the Hill equation to the increase produced by propafenone at concentrations in the range of  $0.001$ – $1 \mu\text{M}$  and averaged  $12.0 \pm 3.0 \text{ nM}$  and  $42.0 \pm 2.6\%$ , respectively.

We tested whether cell incubation with  $0.5 \mu\text{M}$  propafenone for  $\geq 24 \text{ h}$  could modify  $I_{Kir2.1}$ , since it has been described that prolonged exposition to other drugs can either increase<sup>10</sup> or decrease<sup>19</sup>  $I_{Kir2.1}$  density. However, our results demonstrated that incubation with propafenone  $0.5 \mu\text{M}$  did not modify  $I_{Kir2.1}$  density ( $n = 15$  cells from three different culture dishes,  $P > 0.05$ ; data not shown).

Figure 2A and B shows  $I$ – $V$  curves for  $I_{Kir2.2}$  and  $I_{Kir2.3}$ , respectively. Propafenone ( $0.5 \mu\text{M}$ ) failed to increase both inward and outward currents generated by Kir2.2 and 2.3 channels. These results were further



**Figure 1** Low concentrations of propafenone increase  $I_{Kir2.1}$  in CHO cells. (A)  $I_{Kir2.1}$  traces recorded by applying the protocol shown at the top in the absence and presence of  $0.5 \mu\text{M}$  propafenone. (B) Normalized  $I_{Kir2.1}$  recorded at  $-120$  and  $-50 \text{ mV}$  during control recordings, after beginning the propafenone ( $0.5 \mu\text{M}$ ) perfusion and, finally, following the washout of the drug with drug-free solution ( $n = 7$ ). The arrows represent the beginning and the end of perfusion with the propafenone-containing solution. (C and D)  $I$ – $V$  curves for currents measured at the end of the pulses in the absence and presence of propafenone  $0.5$  (C) ( $n = 7$ ) and  $1 \mu\text{M}$  (D) ( $n = 12$ ). The insets show data at potentials positive to  $E_K$  on an expanded scale. \* $P < 0.05$  vs. control. (E) Percentage of  $I_{Kir2.1}$  increase at  $-50 \text{ mV}$  as a function of propafenone concentrations. Continuous line represents the fit of a Hill equation to the data. Each point/bar represents the mean  $\pm$  SEM of greater than or equal to five experiments/cells.

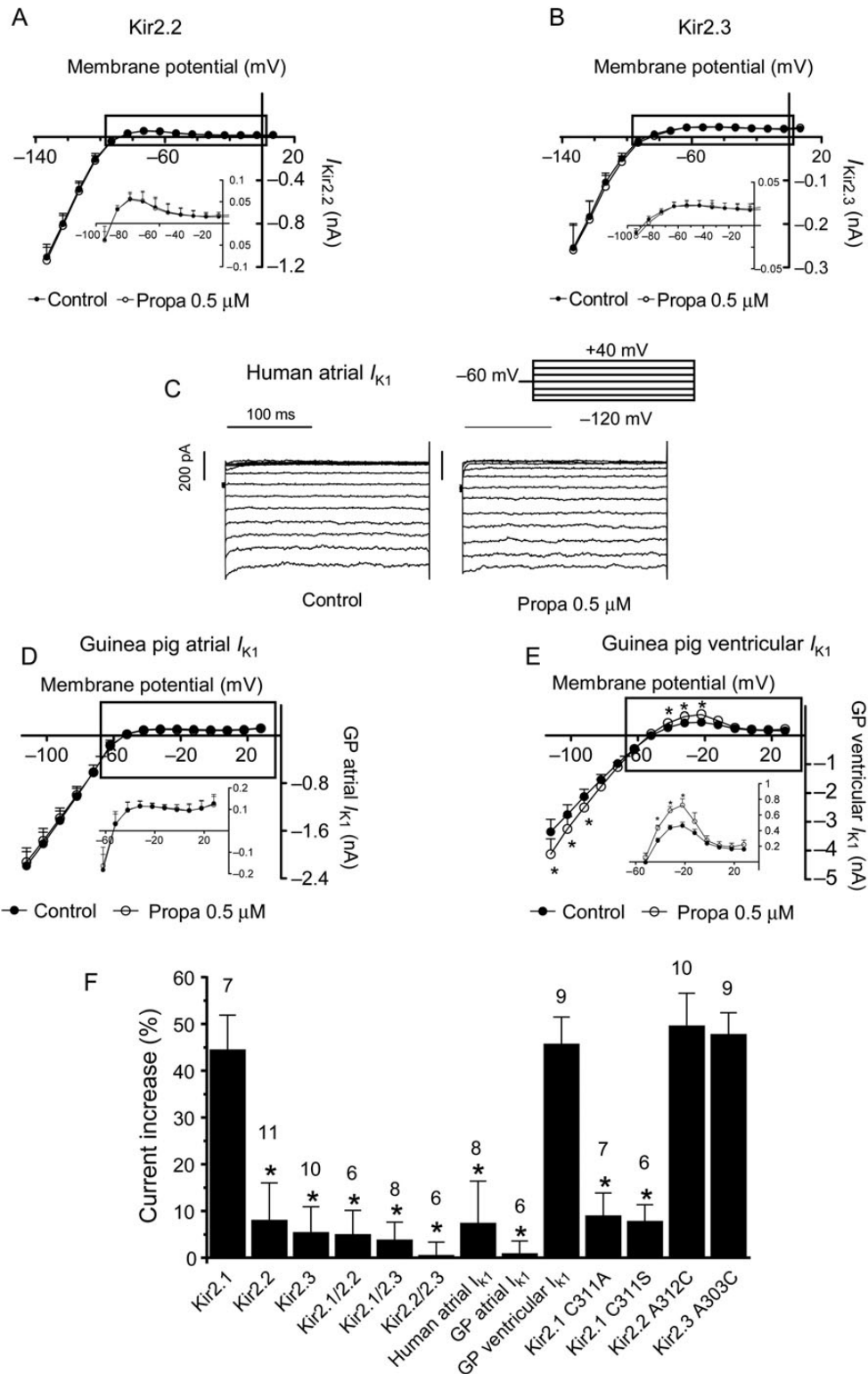


**Figure 2** Low concentrations of propafenone do not modify  $I_{Kir2.2}$  and  $I_{Kir2.3}$  recorded in CHO cells and human atrial  $I_{K1}$ , but increase guinea pig ventricular  $I_{K1}$ . (A and B)  $I$ - $V$  curves for  $I_{Kir2.2}$  (A) ( $n = 11$ ) and  $I_{Kir2.3}$  (B) ( $n = 10$ ) measured at the end of the pulses. The insets show data at potentials positive to  $E_K$  on an expanded scale. (C)  $I_{K1}$  traces recorded by applying the protocol shown at the top in the absence and presence of 0.5  $\mu$ M propafenone in a human atrial myocyte. (D and E)  $I$ - $V$  curves for guinea pig atrial (D) ( $n = 6$ ) and ventricular (E) ( $n = 9$ )  $I_{K1}$  measured at the end of the pulses. The insets show data at potentials positive to  $E_K$  on an expanded scale. In (E),  $*P < 0.05$  vs. control. (F) Percentage of current increase at 40 mV positive to the  $E_K$  produced by 0.5  $\mu$ M propafenone. Numbers over bars represent the number of experiments/cells. In (F),  $*P < 0.05$  vs. Kir2.1. Each point/bar represents the mean  $\pm$  SEM of greater than or equal to six experiments/cells.

confirmed by testing a wide range of propafenone concentrations (0.1 nM–1  $\mu$ M). Furthermore, as mentioned, propafenone significantly inhibited  $I_{Kir2.2}$  and  $I_{Kir2.3}$  at concentrations  $> 1 \mu$ M.<sup>16</sup> We also tested the effects of 0.5  $\mu$ M propafenone on cells cotransfected (0.5:0.5 ratio) with both Kir2.1 and Kir2.2 (Kir2.1/2.2), with Kir2.1 and Kir2.3 (Kir2.1/2.3), and with Kir2.2 and Kir2.3 (Kir2.2/2.3) channels. Kir2.1/2.2 and Kir2.1/2.3 currents displayed activation kinetics significantly different from those of the respective homotetrameric channels, demonstrating the heterotetrameric nature of the channels.<sup>10,16</sup> Figure 2F shows the percentage of propafenone-induced increase in the outward current generated by applying pulses at potentials 40 mV positive to  $E_K$ . Propafenone (0.5  $\mu$ M) failed to increase inward and outward currents generated by heterotetrameric channels ( $P > 0.05$  vs. control, Figure 2F), demonstrating that its effects were only apparent in channels composed of four Kir2.1 subunits.

It is accepted that human atrial  $I_{K1}$  is generated by Kir2.x heterotetramers of unknown composition since all the three Kir2.x clones are present in human atrial tissue.<sup>2</sup> Therefore, we hypothesized that propafenone would fail to modify human atrial  $I_{K1}$ . Figure 2C shows original  $I_{K1}$  recordings obtained in an isolated human atrial myocyte by applying 250 ms pulses from a holding potential of  $-60$  mV to voltages ranging from  $-120$  to  $+40$  mV in the absence and presence of propafenone (0.5  $\mu$ M). Results obtained in eight cells from four different patients confirmed that propafenone did not significantly modify either the inward or outward current (Figure 2F). Since human ventricular preparations were not available, then we compared the effects of propafenone in guinea pig atrial and ventricular cells. Figure 2D demonstrates that 0.5  $\mu$ M propafenone did not modify either inward or outward guinea pig atrial  $I_{K1}$ , whereas it significantly increased both inward and outward ventricular  $I_{K1}$  (Figure 2E). Furthermore, in guinea pig ventricular myocytes,  $I_{K1}$  augmentation was of similar magnitude to that observed in heterologous expression systems (Figure 2F).

As mentioned, flecainide also selectively increases  $I_{Kir2.1}$ , an effect attributed to its binding to Cys311 residue located at the  $\beta$ I strand within the C terminus of the cytoplasmic domain. Moreover, Cys311, which in Kir2.2 and 2.3 channels is an Ala, was critical for explaining the selective effects of flecainide on Kir2.1 over Kir2.2 and 2.3 channels.<sup>10</sup> Since propafenone-increasing effects were only apparent on Kir2.1 channels, we tested whether propafenone also binds to the same binding site as flecainide. For this purpose, we tested the propafenone effects on C311A and C311S channels. Figure 2F shows that propafenone did not increase  $I_{Kir2.1}$  generated by either C311A or C311S. In contrast, substitution of Ala present at position equivalent to Cys311 in both Kir2.2 (A312C) and Kir2.3 (A303C) channels rendered channels sensitive to the propafenone-increasing effects. Indeed, increasing effects produced by 0.5  $\mu$ M propafenone on A312C  $I_{Kir2.2}$  and A303C  $I_{Kir2.3}$  were similar to those produced over  $I_{Kir2.1}$  (Figure 2F).

### 3.2 Propafenone increases Kir2.1 open probability

Figure 3A shows single-channel traces recorded by applying 10 s pulses from 0 to  $-80$  mV in the absence and presence of 0.5  $\mu$ M propafenone. Under control conditions, Kir2.1 channel activity was characterized by few and long events, leading to an opening frequency ( $f_o$ ) of  $2.6 \pm 0.1$  Hz and a mean open probability ( $P_o$ ) of  $0.61 \pm 0.02$  ( $n = 6$ ; Figure 3C and E). Propafenone did not modify either the mean unitary amplitude ( $2.4 \pm 0.01$  pA; Figure 3B and see Supplementary material online, Figure S2), or the slope conductance values ( $\gamma = 29.3 \pm 0.7$  vs.

$30.6 \pm 0.8$  pS,  $P > 0.05$ ), yielded by the fit of a linear function to the single-channel current–voltage relationship. Propafenone did, however, change the channel gating by significantly increasing  $f_o$  (Figure 3C) and mean open time (MOT; Figure 3D), which resulted in a significant increase of the  $P_o$  ( $P < 0.05$ ,  $n = 6$ ; Figure 3E). In fact, it increased the  $P_o$  at all the potentials tested (range  $-100$  to  $-40$  mV).

### 3.3 Propafenone decreases outward rectification by decreasing polyamines affinity of Kir2.1 channels

Augmenting effects produced by propafenone were significantly more marked at potentials positive than at potentials negative to the  $E_K$ . To analyse the putative propafenone effects on Kir2.1 outward rectification in more detail, the degree of rectification of Kir2.1 channels was estimated as the relative chord conductance ( $G_C$ ). Figure 4A shows the relative  $G_C$  in the absence and presence of 0.01 ( $n = 6$ ), 0.1 ( $n = 6$ ), and 0.5  $\mu$ M ( $n = 7$ ) propafenone. Propafenone shifted the midpoint of the curves in a concentration-dependent manner (from  $-91.2 \pm 1.0$  to  $-89.0 \pm 0.3$  and  $-86.0 \pm 1.3$  mV for 0.1 and 0.5  $\mu$ M propafenone, respectively;  $P < 0.05$ ) and decreased the steepness of the rectification as reflected by the reduction in the z-values (from  $3.3 \pm 0.1$  to  $2.8 \pm 0.4$  and  $2.3 \pm 0.3$  for 0.1 and 0.5  $\mu$ M propafenone, respectively;  $P < 0.05$ ).

Since Kir2.1 outward rectification is mainly due to the voltage-dependent block produced by intracellular polyamines, then we tested whether propafenone modified the polyamine affinity of Kir2.1 channels. For this purpose, we assessed the concentration-dependent effects of spermine in the absence and presence of propafenone in excised inside-out macropatches ( $[K^+]_o/[K^+]_i = 140/140$  mM). Figure 4B shows that, under control conditions, spermine inhibited the current recorded at  $+50$  mV in a concentration-dependent manner. This spermine blockade significantly decreased when the polyamine was added in the presence of propafenone (Figure 4B). Figure 4C shows the concentration-dependence of the spermine block ( $IC_{50} = 0.5 \pm 0.1$  nM;  $E_{max} = 92.2 \pm 4.6\%$ ;  $n = 8$ ). Propafenone shifted rightwards the spermine concentration–response curve ( $IC_{50} = 1.1 \pm 0.1$  and  $4.5 \pm 0.1$  nM for 0.1 and 0.5  $\mu$ M propafenone, respectively) and decreased the maximum effect ( $E_{max} = 85.4 \pm 4.7$  and  $81.4 \pm 2.4\%$  for 0.1 and 0.5  $\mu$ M propafenone, respectively;  $P < 0.05$ ,  $n = 8$ ). These results suggested that propafenone decreased the spermine block by a ‘non-competitive’ mechanism. Finally, we analysed the effects of propafenone in Kir2.1 channels with mutations in anionic residues that determine polyamines binding within the transmembrane and the cytoplasmic pore (D172A, E224A, E299A, D259A, and D255R). All these mutations suppressed the outward rectification of Kir2.1 channels and all of them, except D259A, significantly reduced the propafenone-induced  $I_{Kir2.1}$  increase (Figure 4D). Overall, these results suggest that propafenone, like flecainide, selectively increases outward  $I_{Kir2.1}$  by decreasing the channel affinity for polyamines.

### 3.4 Molecular requirements for drugs to increase $I_{Kir2.1}$

Our next goal was to elucidate the chemical requirements for a drug to bind to the Cys311–Kir2.1 binding site. To this end, we first analysed the propafenone interaction with Cys311 using a computational approach by means of AutoDock Vina.<sup>17</sup> Figure 5A shows the binding site of (R)-propafenone into Kir2.1. The latched interface between two Kir2.1 subunits (A in blue and B in yellow) illustrates the critical region of interactions. The results demonstrate that propafenone’s alkyl-phenyl chain establishes a network of hydrophobic interactions with residues belonging



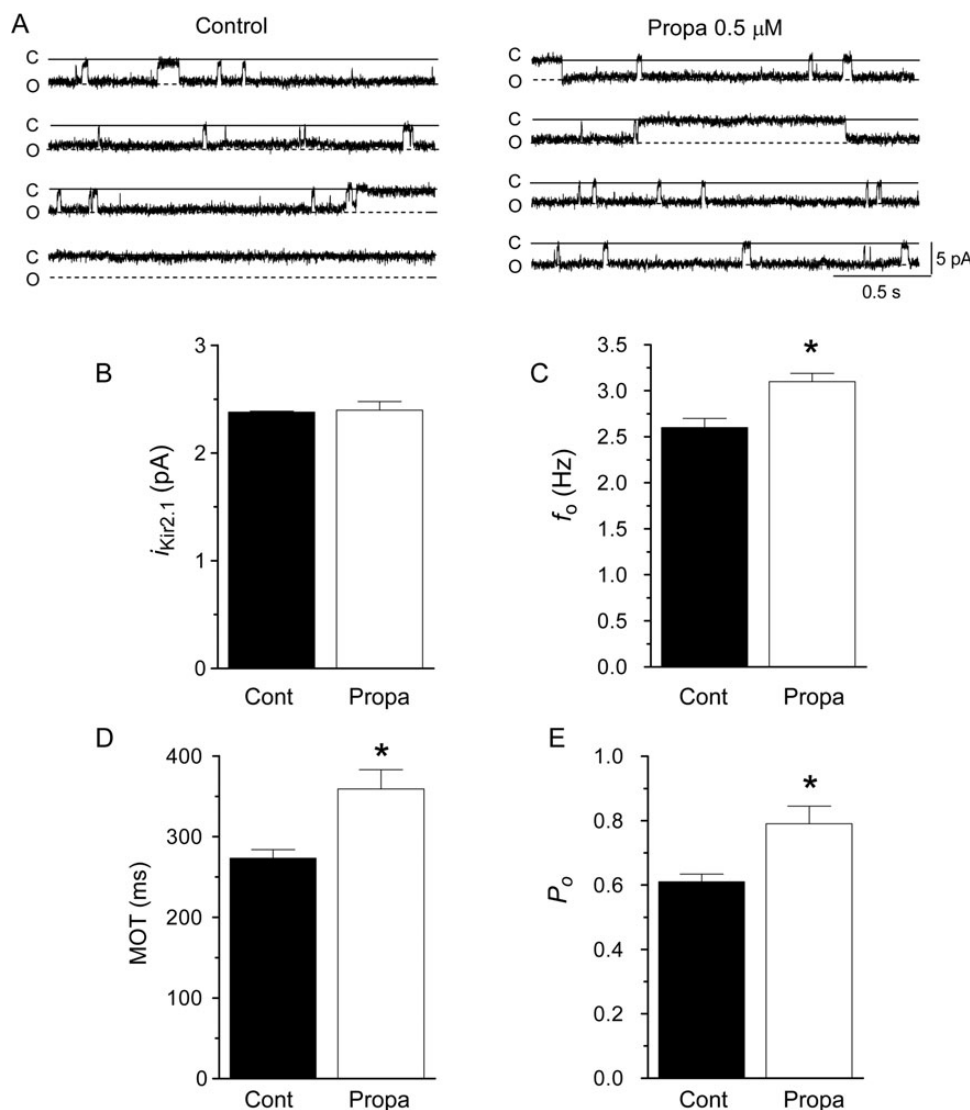


**Figure 3** Effects of propafenone on  $i_{Kir2.1}$ . (A) Single-channel recordings in the absence and presence of propafenone. Closed- and open-channel levels are indicated by C and O, respectively. Unitary current amplitude (B),  $f_o$  (C), MOT (D), and  $P_o$  (E) in the absence and presence of propafenone. Each bar represents the mean  $\pm$  SEM of six experiments/cells. \* $P < 0.05$  vs. control.

to two Kir2.1 neighbouring subunits (Figure 5B). In addition, the Arg67 side chain forms a hydrogen bond with propafenone's carbonyl group (in red in Figure 5B). These interactions could promote the binding orientation of the alkylamino tail allowing the formation of the critical hydrogen bond between propafenone's hydroxyl group and Cys311 (Figure 5A and C). Binding modes of (S)-propafenone, (R)-, and (S)-flecainide were very similar to that predicted for (R)-propafenone. Therefore, they were used as the reference compounds to develop a pharmacophore model for binding to the Kir2.1-binding site.

Overall, it can be proposed that the pharmacophore of drugs that interact with Cys311 must present an 'L-like' configuration with a 'short' and a 'long arm' linked by an aromatic ring (Figure 5D). The angle between the two arms must be of  $\approx 100^\circ$ . The hydrogen bond acceptor/donor group, which is actually the one that interacts with Cys311, must be located in the 'short arm' within a critical distance in the range of 5.1–5.7 Å. In addition, at the end of the 'long arm' (7.5–7.7 Å), a hydrophobic group must be present. This hydrophobic group

will be embedded in a 'hydrophobic pocket' formed by the lateral chains of Val194, Leu217, Tyr341, Phe344, and His345 belonging to subunit A. Interestingly, residues of the neighbouring subunit also contribute to the pocket (Figure 5D). Finally, an additional hydrogen bond between either Arg67 or Glu63 and the drug is critical for the drug stabilization in the proper interacting position.

To test this hypothesis, we investigated drugs that either met or not met the structural requirements predicted in this pharmacophore. To this end, we used the ligand-based pharmacophore as a 3D query for searching for compounds in chemical databases. Among those that did not meet the requirements, we selected atenolol and dronedarone. As mentioned, the chemical structure of atenolol is closely related to that of propafenone (see Supplementary material online, Figure S3); however, it lacks the hydrophobic domain at the end of the long arm. Figure 6A demonstrates that atenolol (1 nM–1  $\mu$ M) did not modify either outward or inward  $I_{Kir2.1}$ . It has been previously demonstrated that dronedarone, the amiodarone's chemical analogue, inhibits

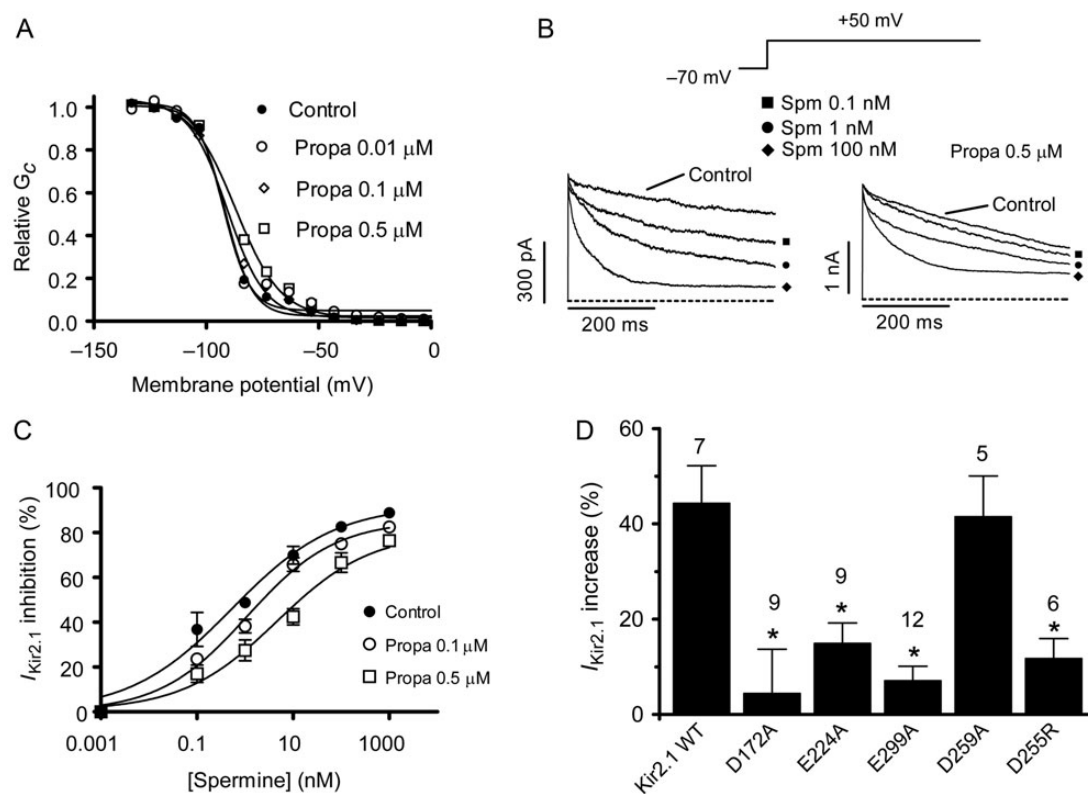


**Figure 4** Propafenone decreases Kir2.1 channel affinity for polyamines. (A) Mean relative  $G_C$  under control conditions and in the presence of propafenone. Solid lines represent the fit of a Boltzmann function to the data. (B) Current traces recorded at +50 mV in excised inside-out patches from HEK-293 cells expressing Kir2.1 channels under control conditions and after cytoplasmic surface application of spermine (Spm) in the absence and presence of propafenone. Dashed lines represent the zero current level. (C) Percentage of current inhibition at +50 mV in excised inside-out patches as a function of Spm concentrations in the absence and presence of propafenone. Solid lines represent the fit of a Hill equation to the data. (D) Percentage of current increase at +50 mV produced by propafenone on Kir2.1 WT and mutated channels. Numbers over bars represent the number of experiments/cells. Throughout Figure 4, each point/bar represents the mean  $\pm$  SEM of greater than or equal to five experiments/cells. \* $P < 0.05$  vs. Kir2.1 WT.

cardiac  $I_{K1}$  at micromolar concentrations.<sup>20</sup> However, the putative effects of dronedarone on  $I_{Kir2.1}$  at therapeutically relevant concentrations have not been reported yet. Dronedarone neither presents an 'L-like' structure nor is properly sized to meet the pharmacophore characteristics. Figure 6B shows that, as predicted, dronedarone 1–100 nM did not modify inward and outward  $I_{Kir2.1}$ .

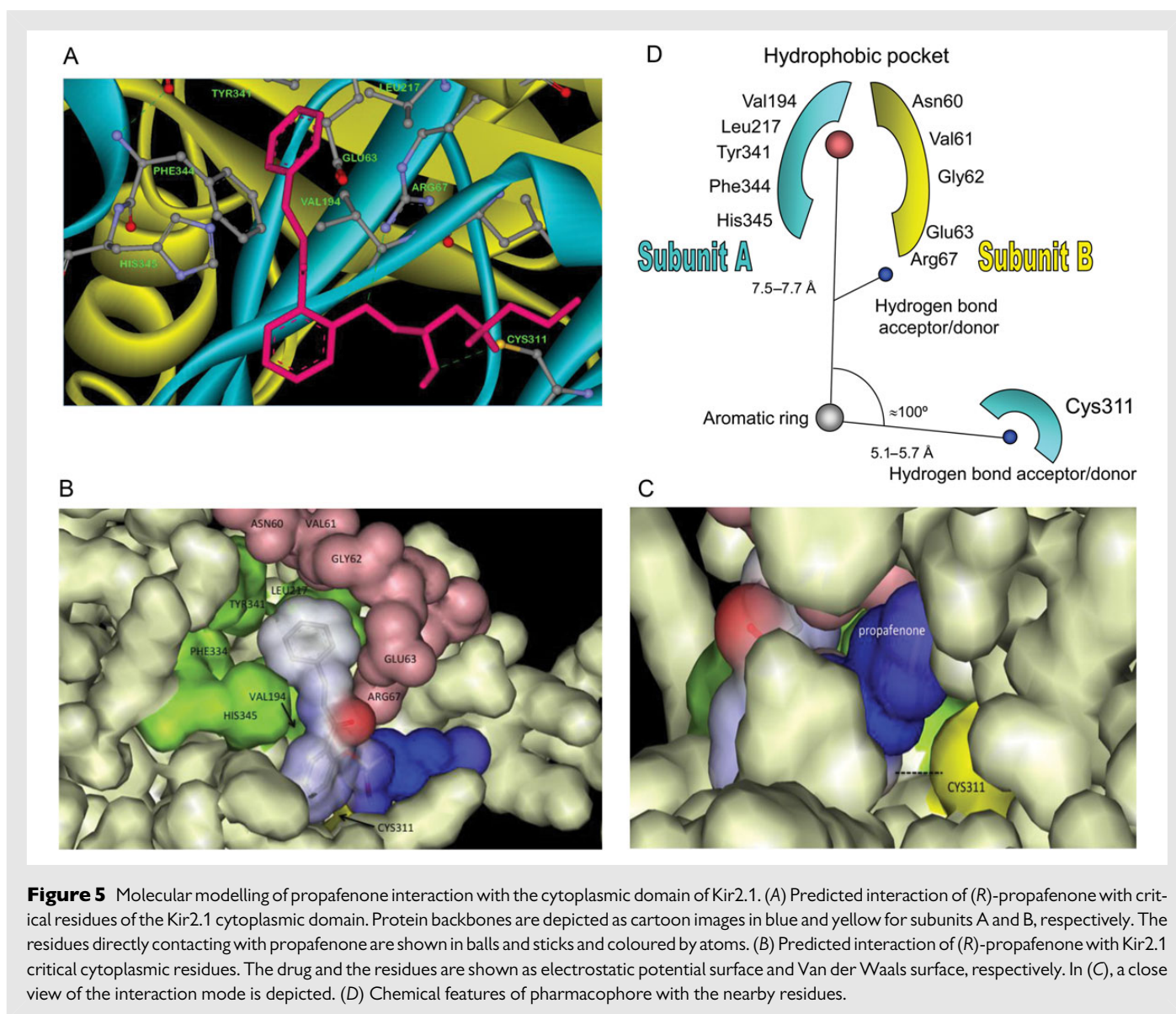
Among those drugs that meet the criteria of the pharmacophore we selected timolol, another  $\beta_1$ -adrenoceptor antagonist. As can be observed in Supplementary material online, Figure S3, timolol exhibits an 'L-like' type structure with electronegative and hydrophobic groups in its short and long arms, respectively. Indeed, oxygen of the six-membered timolol's ring formed a hydrogen bond with Cys311. In agreement with the computational prediction, timolol increased outward  $I_{Kir2.1}$  (Figure 6C) in a concentration-dependent manner (Figure 6D), being very potent for this effect ( $3.2 \pm 0.3$  nM). Furthermore, we tested if these increasing effects were due to its interaction with Cys311 by analysing its effects on C311A Kir2.1 channels. In these channels, timolol 1 nM did not modify the outward current at +50 mV ( $3.5 \pm 1.6\%$  increase,  $n = 5$ ,  $P > 0.05$ ).

## 4. Discussion

Our current results demonstrate that propafenone binds to Cys311, thereby decreasing the channels affinity for polyamines, an effect that

increases outward  $I_{Kir2.1}$  by reducing the inward rectification. These effects were quite similar to those produced by flecainide.<sup>10</sup> Therefore, we hypothesized that Kir2.1 channels contain a high-affinity-binding site for these compounds. Drug binding to Cys311 at the  $\beta_1$  strand of the cytoplasmic domain of Kir2.1 channels increases the current generated by Kir2.1 homotetramers.

Our results demonstrate that propafenone and flecainide share a common binding site within Kir2.1 channels determined by Cys311, which is absent in Kir2.2 and 2.3 channels. Indeed, the C311A mutation in Kir2.1 channels abolished the propafenone-increasing effects, while Cys incorporation in both Kir2.2 (A312C) and Kir2.3 (A303C) rendered the channels sensitive to propafenone. Drug binding to Cys311 allosterically decreased Kir2.1 channel affinity for polyamines. Of interest, propafenone did not decrease binding of polyamines to their cytoplasmic and transmembrane pore-binding sites in a competitive manner, but rather induced a non-competitive antagonism. As a result, propafenone decreased channel rectification, an effect that, in turn, markedly increased the current generated at potentials positive to the  $E_K$ . Simultaneously, at potentials negative to the  $E_K$ , propafenone increased  $f_o$  and MOT, leading to an increase in the channel  $P_o$  at all the voltages tested without modifying the single-channel current amplitude. Increasing effects produced by propafenone at potentials negative to the  $E_K$  share common characteristics with the increasing effects produced by PIP<sub>2</sub>. These results suggest that propafenone increases  $I_{Kir2.1}$  by



enhancing the PIP<sub>2</sub> activating effects. Enhancement of the PIP<sub>2</sub> activating effects might explain the propafenone-increasing effects produced at membrane potentials negative to the E<sub>K</sub>, which were apparent with only two of the concentrations tested. It is interesting to note that propafenone binding to Cys311 produces an apparent dissociation of channel affinity for polyamines and PIP<sub>2</sub> since it decreases and increases the channel affinity for polyamines and PIP<sub>2</sub>, respectively. Indeed, it has been demonstrated that polyamines act as positive cofactors of PIP<sub>2</sub> binding to Kir2.x channels.<sup>21</sup> The precise mechanism by which binding of propafenone modifies channel affinity for polyamines and PIP<sub>2</sub> remains to be elucidated. Our results stress the importance of the cytoplasmic Kir2.1 domain in the control of the channel gating and demonstrate further that current through inward rectifier channels can be modulated by drug binding to this cytoplasmic domain. In fact, while Kir2.1 channels exhibit two different propafenone binding sites at the cytoplasmic domain, none of them are located into the pore. The low-affinity-binding site (determined by Arg228 and Arg260) is responsible for the propafenone blocking effects (IC<sub>50</sub> = 52 μM),<sup>16</sup> whereas the high-affinity-binding site (determined by Cys311) is responsible for the increasing effects. Of interest, affinities of the Kir2.1 increasing

drugs identified so far are remarkably high since they are in the low nanomolar range.

Here, we identified the 'pharmacophore', i.e. the abstract description of molecular features necessary for molecular recognition of a ligand by the Kir2.1 β1-binding site. Results obtained using a chemical computational approach suggest that drugs that bind to Cys311 present an 'L-like' configuration. In their short arm, they must present a hydrogen bond acceptor/donor allowing the interaction with Cys311. In addition, in their 'long arm', they have to exhibit a lipophilic group, which interacts with the hydrophobic pocket formed by the lateral chains of Leu, Val, Tyr, Phe, and His residues of one of the subunits, as well as, with residues of the neighbouring subunit. Additional anchoring with another hydrogen bond in the region of the junction between the two arms would also stabilize the drug binding.

#### 4.1 Putative electrophysiological implications

The experiments presented here were performed at room temperature, which can be a potential limitation of the study. Overall,



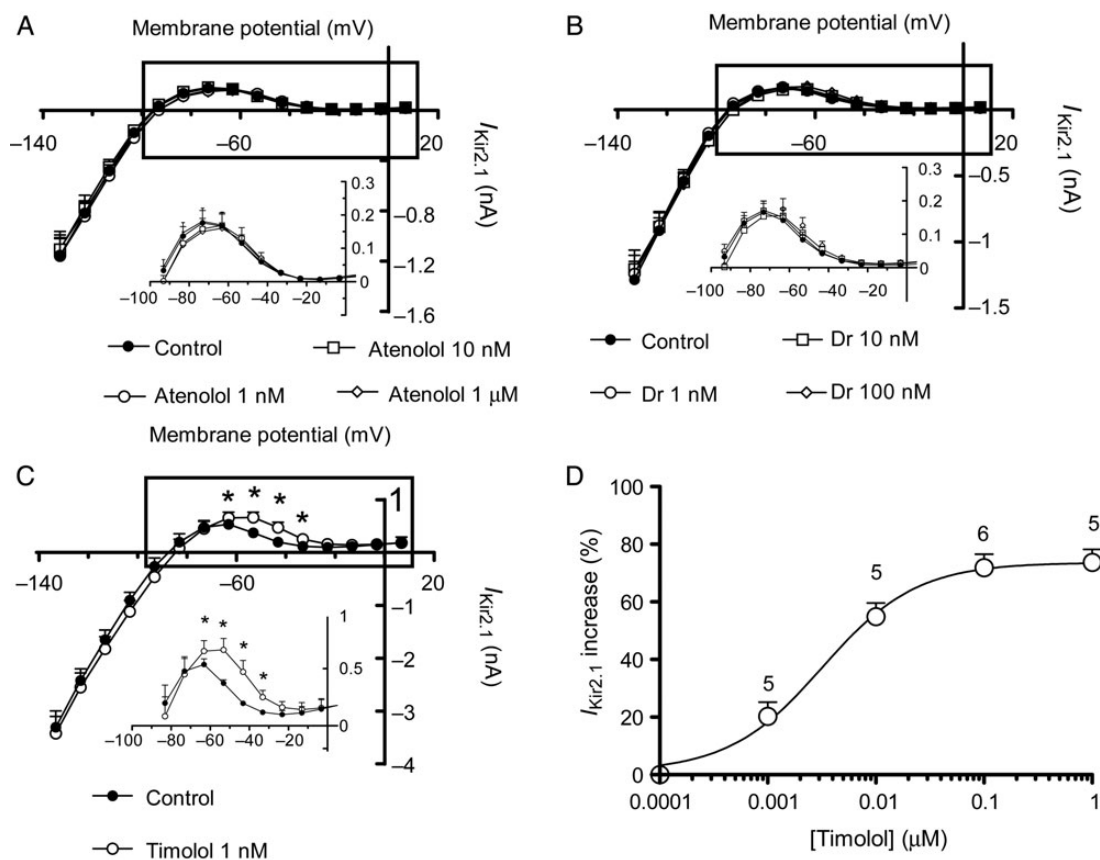


**Figure 6** Effects of drugs that meet or not the Cys311 binding-drug pharmacophore. (A–C)  $I-V$  curves for currents measured at the end of the pulses in the absence and presence of atenolol (A) ( $n = 5$ ), dronedarone (Dr, B) ( $n = 14$ ), and timolol (C) ( $n = 5$ ). The insets show data at potentials positive to  $E_K$  on an expanded scale. (D) Percentage of  $I_{Kir2.1}$  increase at  $-50$  mV as a function of several timolol concentrations. Continuous line represents the fit of a Hill equation to the data. Each point represents the mean  $\pm$  SEM of greater than or equal to five experiments/cells.

however, our results demonstrated that propafenone, like flecainide, the two drugs used for the acute cardioversion of AF, increases the current generated by Kir2.1 homotetramers at therapeutically relevant concentrations. Consistently with this conclusion, propafenone did not increase human atrial  $I_{K1}$ , confirming previous observations<sup>22</sup>, thereby adding further support to the hypothesis that channels that generate the current consist of heterotetramers in which Kir2.2 and/or Kir2.3 subunits are present.<sup>2</sup> Moreover, the results demonstrate that propafenone does not modify guinea pig atrial  $I_{K1}$ , while it significantly increased the ventricular current. Unfortunately, it was not possible to study human ventricular samples to test whether propafenone is able to increase ventricular  $I_{K1}$ . Should this occur, the propafenone-induced increase of  $I_{K1}$  could contribute to its ventricular proarrhythmic effects,<sup>11</sup> which are particularly apparent in patients with coronary artery disease and/or heart failure.

A drug-induced  $I_{K1}$  increase can be considered a double-edged sword since it may exert pro- or antiarrhythmic effects depending on the myocardial electrical context. An  $I_{K1}$  increase has been proposed to be proarrhythmogenic, since it enhances the occurrence and stability of rotors underlying fibrillatory arrhythmias.<sup>6</sup> Thus, it could be possible that those drugs that bind to Cys311 exert ventricular proarrhythmic effects. Furthermore, these proarrhythmic effects could be enhanced in the presence of tachycardia, since heart rate augmentation increases  $[K]_o$ , which, in turn, increases ventricular  $I_{K1}$ .<sup>23</sup>

On the other hand, it has been proposed that a strong inward rectifying  $I_{K1}$  will counteract DADs, while suppression of  $I_{K1}$  will facilitate them.<sup>24</sup> Indeed, loss-of-function mutations of Kir2.1 channels (Andersen-Tawil Syndrome) lead to instability of the resting membrane potential, DADs, and arrhythmias.<sup>25</sup> In this setting, it has been proposed that the  $I_{K1}$  increase produced by flecainide could contribute to its antiarrhythmic effects in Andersen-Tawil patients.<sup>10,26</sup> Furthermore, it could be speculated that the  $I_{K1}$  increase produced by flecainide<sup>27</sup> and propafenone<sup>28</sup> participates in the control of ventricular arrhythmias in patients with catecholaminergic polymorphic ventricular tachycardia, an hypothesis that merits further analysis. Finally, pure  $I_{Kir2.1}$  increasing drugs, but not propafenone and flecainide, could be of interest for the prevention of DADs in patients with heart failure-induced  $I_{K1}$  decrease.<sup>29</sup>

Proarrhythmic effects of cardiovascular and noncardiovascular drugs have been recognized as an important source of severe adverse drug reactions. There are several mechanisms underlying proarrhythmia, including potent blockade of  $Na^+$  and L-type  $Ca^{2+}$  channels, which can lead to intracardiac conduction disturbances and bradyarrhythmia.<sup>30</sup> Furthermore, it has been extensively demonstrated that rapid component of the delayed rectifier current ( $I_{Kr}$ ) inhibitors (HERG channel blockers) prolongs ventricular APD and the QT interval and may cause polymorphic ventricular tachycardia termed *torsades de pointes* that can degenerate into ventricular fibrillation and sudden cardiac death.<sup>31</sup> In the present study, we have unravelled the pharmacophore

of drugs that bind to Kir2.1 Cys311. We surmise that drugs that enhance  $I_{Kir2.1}$  could exert ventricular proarrhythmic effects, and thus, we propose that binding to Kir2.1 Cys311 is a supplementary mechanism that may underlie drug-induced proarrhythmia. Chamber-specific proarrhythmic effects produced by propafenone and flecainide could be partially attributed to their  $I_{Kir2.1}$  increasing effects.

In summary, we identified the molecular determinants that allow drugs to increase  $I_{Kir2.1}$  by binding to Cys311. Further studies with other drugs are needed to challenge this hypothesis and to confirm their putative profibrillatory and/or antiarrhythmic actions.

## Supplementary material

Supplementary material is available at *Cardiovascular Research* online.

## Acknowledgements

We thank Sandra Sacristán and Paloma Vaquero for their invaluable technical assistance.

**Conflict of interest:** none declared.

## Funding

This work was supported by Ministerio de Ciencia e Innovación (SAF2011-30088 and SAF2011-30112), Instituto de Salud Carlos III (Red HERACLES RD06/0009, Red Investigación Cardiovascular RD12/0042/0011, and PI11/01030), Centro Nacional de Investigaciones Cardiovasculares (CNIC-13 and CNIC-08-2009), Comunidad Autónoma de Madrid (S2010/BMD-2374), and Sociedad Española de Cardiología grants.

## References

- Anumonwo JM, Lopatin AN. Cardiac strong inward rectifier potassium channels. *J Mol Cell Cardiol* 2010;**48**:45–54.
- Gaborit N, Le Bouter S, Szuts V, Varro A, Escande D, Nattel S, Demolombe S. Regional and tissue specific transcript signatures of ion channel genes in the non-diseased human heart. *J Physiol* 2007;**582**:675–693.
- Piao L, Li J, McLerie M, Lopatin AN. Transgenic upregulation of  $I_{K1}$  in the mouse heart is proarrhythmic. *Basic Res Cardiol* 2007;**102**:416–428.
- Samie FH, Berenfeld O, Anumonwo J, Mironov SF, Udassi S, Beaumont J, Taffet S, Pertsov AM, Jalife J. Rectification of the background potassium current: a determinant of rotor dynamics in ventricular fibrillation. *Circ Res* 2001;**89**:1216–1223.
- Warren M, Guha PK, Berenfeld O, Zaitsev A, Anumonwo JM, Dharmoon AS, Bagwe S, Taffet SM, Jalife J. Blockade of the inward rectifying potassium current terminates ventricular fibrillation in the guinea pig heart. *J Cardiovasc Electrophysiol* 2003;**14**:621–631.
- Pandit SV, Jalife J. Rotors and the dynamics of cardiac fibrillation. *Circ Res* 2013;**112**:849–862.
- Voigt N, Trausch A, Knaut M, Matschke K, Varró A, Van Wagoner DR, Nattel S, Ravens U, Dobrev D. Left-to-right atrial inward rectifier potassium current gradients in patients with paroxysmal versus chronic atrial fibrillation. *Circ Arrhythm Electrophysiol* 2010;**3**:472–480.
- Deo M, Ruan Y, Pandit SV, Shah K, Berenfeld O, Blaufox A, Cerrone M, Noujaim SF, Denegri M, Jalife J, Priori SG. KCNJ2 mutation in short QT syndrome 3 results in atrial fibrillation and ventricular proarrhythmia. *Proc Natl Acad Sci USA* 2013;**110**:4291–4296.
- Sipido KR, Bito V, Antoons G, Volders PG, Vos MA. Na/Ca exchange and cardiac ventricular arrhythmias. *Ann N Y Acad Sci* 2007;**1099**:339–348.
- Caballero R, Dolz-Gaitón P, Gómez R, Amorós I, Barana A, González de la Fuente M, Osuna L, Duarte J, López-Izquierdo A, Moraleda I, Gálvez E, Sánchez-Chapula JA, Tamargo J, Delpón E. Flecainide increases Kir2.1 currents by interacting with cysteine 311, decreasing the polyamine-induced rectification. *Proc Natl Acad Sci USA* 2010;**107**:15631–15636.
- Bryson HM, Palmer KJ, Langtry HD, Fitton A. Propafenone. A reappraisal of its pharmacology, pharmacokinetics and therapeutic use in cardiac arrhythmias. *Drugs* 1993;**45**:85–130.
- Wadworth AN, Murdoch D, Brogden RN. Atenolol. A reappraisal of its pharmacological properties and therapeutic use in cardiovascular disorders. *Drugs* 1991;**42**:468–510.
- Tamargo J, López-Farré A, Caballero R, Delpón E. Dronedarone. *Drugs Today* 2011;**47**:109–133.
- González de la Fuente M, Barana A, Gómez R, Amorós I, Dolz-Gaitón P, Sacristán S, Atienza F, Pita A, Pinto Á, Fernández-Avilés F, Caballero R, Tamargo J, Delpón E. Chronic atrial fibrillation up-regulates  $\beta$ 1-adrenoceptors affecting repolarizing currents and action potential duration. *Cardiovasc Res* 2013;**97**:379–388.
- Gómez R, Caballero R, Barana A, Amorós I, Calvo E, López JA, Klein H, Vaquero M, Osuna L, Atienza F, Almendral J, Pinto A, Tamargo J, Delpón E. Nitric oxide increases cardiac  $I_{K1}$  by nitrosylation of cysteine 76 of Kir2.1 channels. *Circ Res* 2009;**105**:383–392.
- Amorós I, Dolz-Gaitón P, Gómez R, Matamoros M, Barana A, de la Fuente MG, Núñez M, Pérez-Hernández M, Moraleda I, Gálvez E, Iriepa I, Tamargo J, Caballero R, Delpón E. Propafenone blocks human cardiac Kir2.x channels by decreasing the negative electrostatic charge in the cytoplasmic pore. *Biochem Pharmacol* 2013;**86**:267–278.
- Trott O, Olson AJ. AutoDock Vina: improving the speed and accuracy of docking with a new scoring function, efficient optimization, and multithreading. *J Comput Chem* 2010;**31**:455–461.
- Brooks BR, Bruccoleri RE, Olafson BD, States DJ, Swaminathan S, Karplus M. CHARMm, a program for macromolecular energy, minimization, and dynamics calculations. *J Comput Chem* 1983;**4**:187–217.
- de Boer TP, Nalos L, Stary A, Kok B, Houtman MJ, Antoons G, van Veen TA, Beekman JD, de Groot BL, Ophof T, Rook MB, Vos MA, van der Heyden MA. The anti-protozoal drug pentamidine blocks KIR2.x-mediated inward rectifier current by entering the cytoplasmic pore region of the channel. *Br J Pharmacol* 2010;**159**:1532–1541.
- Gautier P, Guillemare E, Marion A, Bertrand JP, Tourneur Y, Nisato D. Electrophysiological characterization of dronedarone in guinea pig ventricular cells. *J Cardiovasc Pharmacol* 2003;**41**:191–202.
- Xie LH, John SA, Ribale B, Weiss JN. Long polyamines act as cofactors in PIP<sub>2</sub> activation of inward rectifier potassium (Kir2.1) channels. *J Gen Physiol* 2005;**126**:541–549.
- Voigt N, Rozmaritsa N, Trausch A, Zimniak T, Christ T, Wettwer E, Matschke K, Dobrev D, Ravens U. Inhibition of  $I_{K_{ACH}}$  current may contribute to clinical efficacy of class I and class III antiarrhythmic drugs in patients with atrial fibrillation. *Naunyn-Schmiedeberg Arch Pharmacol* 2010;**381**:251–259.
- Hume JR, Uehara A. Ionic basis of the different action potential configurations of single guinea-pig atrial and ventricular myocytes. *J Physiol* 1985;**368**:525–544.
- Pogwizd SM, Schlotthauer K, Li L, Yuan W, Bers DM. Arrhythmogenesis and contractile dysfunction in heart failure: roles of sodium-calcium exchange, inward rectifier potassium current, and residual  $\beta$ -adrenergic responsiveness. *Circ Res* 2001;**88**:1159–1167.
- Tristani-Firouzi M, Etheridge SP. Kir2.1 channelopathies: the Andersen-Tawil syndrome. *Pflugers Arch* 2010;**460**:289–294.
- Fox DJ, Klein GJ, Hahn A, Skanes AC, Gula LJ, Yee RK, Subbiah RN, Krahn AD. Reduction of complex ventricular ectopy and improvement in exercise capacity with flecainide therapy in Andersen-Tawil syndrome. *Europace* 2008;**10**:1006–1008.
- van der Werf C, Kannankeril PJ, Sacher F, Krahn AD, Viskin S, Leenhardt A, Shimizu W, Sumitomo N, Fish FA, Bhuiyan ZA, Willems AR, van der Veen MJ, Watanabe H, Laborde J, Haïssaguerre M, Knollmann BC, Wilde AA. Flecainide therapy reduces exercise-induced ventricular arrhythmias in patients with catecholaminergic polymorphic ventricular tachycardia. *J Am Coll Cardiol* 2011;**57**:2244–2254.
- Hwang HS, Hasdemir C, Laver D, Mehra D, Turhan K, Faggioni M, Yin H, Knollmann BC. Inhibition of cardiac Ca<sup>2+</sup> release channels (RyR2) determines efficacy of class I antiarrhythmic drugs in catecholaminergic polymorphic ventricular tachycardia. *Circ Arrhythm Electrophysiol* 2011;**4**:128–135.
- Janse MJ. Electrophysiological changes in heart failure and their relationship to arrhythmogenesis. *Cardiovasc Res* 2004;**61**:208–217.
- Tamargo J, Delpón E. Pharmacologic bases of antiarrhythmic therapy. In: Zipes D, Jalife J, eds. *Cardiac Electrophysiology*. 6th edn. Philadelphia: Elsevier Saunders, 2014. P. 529–540.
- Tamargo J. Drug-induced torsade de pointes: from molecular biology to bedside. *Jpn J Pharmacol* 2000;**83**:1–19.